An efficient approach to reliability-based topology optimization of continuum structures with multimodal distributions

Zhenzeng Lei
Graduate Student, Dept. of Engineering Mechanics, Dalian University of Technology, Dalian, China
Dixiong Yang
Professor, Dept. of Engineering Mechanics, Dalian University of Technology, Dalian, China

ABSTRACT: In practical applications, some random variables follow multimodal distributions, thus, the corresponding reliability-based topology optimization (RBTO) should be considered. However, conventional reliability analysis methods usually result in large computational error in this case. Therefore, this paper proposes an efficient approach to RBTO of continuum structures with multimodal distributions combining sequential approximate integer programming with trust region (SAIP-TR) and direct probability integral method (DPIM). Firstly, the DPIM is suggested to estimate the failure probability and its sensitivity for the structure involving random variables with multimodal distributions. Secondly, discrete variable topology optimization based on the SAIP-TR is adopted to obtain clear topology configurations. Moreover, since the optimal design in the initial stages will not fail, a two-phase strategy is proposed. In the first phase, a deterministic topology optimization is carried out with the worst-case as the constraint. In the second phase, the optimized result of the first phase is taken as the initial design to perform the RBTO. To reduce the number of structural analyses, only a part of representative points that contribute more to the calculation of failure probability and sensitivity analysis are concerned in each optimization process. Finally, several numerical examples illustrate the high efficiency and accuracy of the proposed approach for RBTO, and exhibit the significant difference between the results of the RBTO considering multimodal distributions and unimodal distributions.

1. INTRODUCTION

Reliability-based topology optimization (RBTO), which considers uncertainties through the failure probability and seeks to a desired design satisfying a specific risk and target reliability level (Maute 2014), has gotten more and more attentions. In fact, there are many practical projects involving random variables that follow multimodal distributions. Consequently, it is essential to consider the RBTO problems with multimodal distributions.

Among the existing works of the RBTO, the mostly used reliability analysis method is the first order reliability method (FORM), especially the performance measurement approach (PMA). In addition, the second order reliability method (SORM) is also a common reliability analysis method in the RBTO. For more details, the interested readers can further refer to the review literatures of reliability-based design (Valdebenito and Schuëller 2010; Yao et al. 2011).

However, these conventional methods are no longer appropriate for the RBTO considering multimodal distributions, because they need to transform multimodal random variables into standard normal space, which will increase the nonlinearity of the limit-state function (Hu and Du 2019). To date, only a few works (Li et al. 2021; Lim and Manuel 2021; Meng et al. 2020; Zhang et al. 2020) have been presented to calculate failure probabilities under multimodal distributions, in which the direct probability integration method (DPIM) provided an efficient and applicable way for calculating the failure probability of multimodal distributions, regardless of whether the performance function is linear or nonlinear (Li et al. 2021). Hence, it is

attractive to introduce the DPIM into the RBTO problems involving multimodal distributions.

Moreover, discrete variable topology optimization can obtain a clear topology configuration and is more suitable for manufacturing (Liu and Ma 2016). Thus, the optimized designs obtained by the framework of reliability-based discrete variable topology optimization (RBDVTO) will significantly facilitate engineering manufacturing. Meanwhile, a robust discrete variable topology optimization algorithm is crucial for the implementation of the RBDVTO. Recently, a novel discrete variable topology optimization algorithm, sequential approximate integer programming with trust region (SAIP-TR), was well used in a variety of topology optimization problems (Liang et al. 2020), demonstrating its strong adaptability. As a result, this approach enables us achieve a satisfactory solution for the RBDVTO problems.

In this study, a RBDVTO framework is developed for continuum structures with multimodal distributions, which is based on the SAIP-TR and the DPIM. Due to the merit of SAIP-TR, the optimal design in the initial stages will not fail so that an efficient two-phase approach is proposed to reduce the computational cost. In the first phase, a deterministic topology optimization is carried out with the worst-case as the constraint until the performance function corresponding to the intermediate design reaches the predefined threshold. In the second phase, the optimized result of the first phase is taken as the initial design to perform the RBTO. To further reduce the number of structural analyses, only a part of the representative points is considered in each optimization process, which relies on the finding that structural compliance maintains a roughly monotonically decreasing trend over the whole optimization process. Finally, the high accuracy and efficiency of the proposed method are verified by numerical examples.

2. RBDVTO VIA DPIM AND SAIP-TR

2.1. Problem formulation

Herein, the minimum structural volume design subject to a given constraint on failure probability is considered. Based on the SAIP-TR, the initial design is chosen as full material and the optimized designs in the first few optimization iterations will not fail. Therefore, a two-phase strategy is adopted to reduce the computational cost, i.e., the minimum structural volume design under the constraint of the compliance is preformed first, and then the RBTO is carried out when the structure fails. Specifically, the following two types subproblems are implemented respectively.

$$
\begin{aligned}
&\min_{\boldsymbol{\rho}} \ V=\sum_{e=1}^{M}\rho_e^k V_e \\
&\text{s.t.} \quad \mathbf{KU}=\mathbf{F} \\
&\quad C(\boldsymbol{\rho}) \approx \max\left[C\left(\boldsymbol{\rho},\boldsymbol{\theta}_q\right)\right]+ \\
&\qquad \sum_{e=1}^{M}\frac{\partial\left\{\max\left[C\left(\boldsymbol{\rho}^k,\boldsymbol{\theta}_q\right)\right]\right\}}{\partial\rho_e}\left(\rho_e-\rho_e^k\right)\le \bar{C} \\
&\quad \sum_{e=1}^{M} c_e\left(\rho_e-\rho_e^k\right)\le r_k \quad c_e=\{-1,1\} \\
&\quad \rho_e\in\{0,1\},\ \ e=1,2,\ldots,M
\end{aligned}
\tag{1}
$$

$$
\begin{aligned}
&\min_{\boldsymbol{\rho}} \ V=\sum_{e=1}^{M}\rho_e^k V_e \\
&\text{s.t.} \quad \mathbf{K}\left(\boldsymbol{\rho},\boldsymbol{\Theta}\right)\mathbf{U}=\mathbf{F}\left(\boldsymbol{\Theta}\right) \\
&\quad P_f\left(\boldsymbol{\rho}\right)\approx P_f^{\mathrm{DPIM}}\left(\boldsymbol{\rho}^k\right) \\
&\qquad +\sum_{e=1}^{M}\frac{\partial P_f^{\mathrm{DPIM}}}{\partial\rho_e}\left(\rho_e-\rho_e^k\right)\le \bar{P} \\
&\quad \sum_{e=1}^{M} c_e\left(\rho_e-\rho_e^k\right)\le r_k \quad c_e=\{-1,1\} \\
&\quad \rho_e\in\{0,1\},\ \ e=1,2,\ldots,M
\end{aligned}
\tag{2}
$$

where, the compliance constraint in (1) is the worst-case, i.e. the maximum value of $C(\boldsymbol{\rho}, \boldsymbol{\theta}_q)$, the penultimate term in (1) or (2) is the trust region constraint, the parameter r_k is the trust region radius of the k-th subproblem.

The failure probability estimated by the DPIM in (2) is expressed as

$$
P_f^{\mathrm{DPIM}}\left(\boldsymbol{\rho}\right)\approx\sum\nolimits_{q=1}^{N}\mathcal{H}\left[-g\left(\boldsymbol{\rho},\boldsymbol{\theta}_q\right)\right]\cdot P_q \tag{3}
$$

where N is the total number of representative points that are adopted to partition the input probability space, P_q is the assigned probability of the q-th representative point and $\mathcal{H}[\cdot]$ denotes the Heaviside function. $g(\boldsymbol{\rho}, \boldsymbol{\theta}_q)$ is the performance function

$$g(\boldsymbol{\rho},\boldsymbol{\theta}_q)=\bar{C}-C(\boldsymbol{\rho},\boldsymbol{\theta}_q) \tag{4}$$

where, $C(\boldsymbol{\rho}, \boldsymbol{\theta}_q)$ is the structural compliance, and its prescribed threshold is $\bar{C}$.

Moreover, the Gaussian mixture model (Figueiredo and Jain 2002) is adopted for uncertainty modeling of input random variables with multimodal distributions.

$$p\left(X\middle|\mu,\sigma\right)=\sum_{i=1}^{S}\alpha_i\varphi\left(\frac{X-\mu_i}{\sigma_i}\right) \tag{5}$$

where s denotes the number of Gaussian components, α_i means the weighted coefficient of the i-th Gaussian component, and it satisfies $\alpha_i \geq 0$ and $\sum_{i=1}^{S}\alpha_i = 1$.

2.2. Relaxed strategy of the SAIP-TR

Considering the different convergence of the optimization formulations (1) and (2), two different strategies (Liang et al. 2020) that determine the r_k are implemented respectively. For the deterministic optimization (1), the size of the trust region is fixed at every iteration, that is

$$r_k = \alpha_r M \tag{6}$$

where α_r is a parameter with a small value, and M is the number of elements.

For the optimization (2), the strategy is to adjust the trust region dynamically

$$r_{k+1}=\begin{cases}\min\left\{1.2r_k, r^{\mathrm{U}}\right\}, & \text{if } \bar{\omega}_{k\text{-}1}<0 \text{ and } \bar{\omega}_k<0\\ \max\left\{0.8r_k, r^{\mathrm{L}}\right\}, & \text{if } \bar{\omega}_{k\text{-}1}>0 \text{ and } \bar{\omega}_k>0\\ r_k, & \text{otherwise}\end{cases} \tag{7}$$

where $\bar{\omega}_k$ indicates the reduction or increase of objective function, which is defined as

$$\bar{\omega}_k = V\left(\boldsymbol{\rho}^{k+1}\right)-V\left(\boldsymbol{\rho}^{k}\right) \tag{8}$$

r^{L} and r^{U} denote the lower and upper bounds of the trust region radius, and their values depend on the specific problem. It should be noted that the trust region radius will be updated only when the changes of the objective functions are the same for two successive iterations, which means the trust region expands if the objective function converges stably, and shrinks if the objective function oscillates.

Moreover, to make the subproblem in SAIP-TR feasible, it is necessary to adopt relaxation strategy for the constraint target which dynamically adjusting the constraint threshold during the iterative process is imposed. Because the constraints of (1) and (2) are different, thus, different relaxed strategies are needed. Specifically, for the threshold of compliance, the relaxed strategy is defined as follows

$$\left(\bar{C}\right)^{nc}=\bar{C}-\frac{nc}{\mathrm{NC}}\left[\max\left\{C\left(\boldsymbol{\rho},\boldsymbol{\theta}_q\right)\right\}-\bar{C}\right] \tag{9}$$

where, the range of the maximum value of $C(\boldsymbol{\rho}, \boldsymbol{\theta}_q)$ to the prescribed threshold $\bar{C}$ is divided into NC parts, and nc is the number of relaxations. It indicates that the value of compliance gradually converges to its threshold as the iteration progresses. It is worth noting that formula (9) is utilized to update the value of compliance, only when the objective function of the optimization problem (1) converges.

In addition, the relaxed strategy for the failure probability threshold is defined as

$$\text{if } P_f\left(\boldsymbol{\rho}^k\right)\neq 0,\quad \bar{P}^k=\begin{cases}(1+s)P_f\left(\boldsymbol{\rho}^k\right), & \text{if } (1+s)P_f\left(\boldsymbol{\rho}^k\right)<\bar{P}\\ (1-s)P_f\left(\boldsymbol{\rho}^k\right), & \text{if } (1-s)P_f\left(\boldsymbol{\rho}^k\right)>\bar{P}\\ \bar{P}, & \text{otherwise}\end{cases} \tag{10}$$

$$\text{if } P_f\left(\boldsymbol{\rho}^k\right)=0,\ \bar{P}^k=\frac{1}{L}\sum_{e=1}^{M}\frac{\partial\left[P_f\left(\boldsymbol{\rho}^k\right)\right]}{\partial\rho_e}\rho_e^k \tag{11}$$

where $\bar{P}^k$ represents the threshold of failure probability in the k-th iteration, L is a large number parameter and is set to be 5×10^4, the parameter s is usually a small positive number.

2.3. Sensitivity analysis

As mentioned above, the constraint functions in (1) and (2) are the linear approximation of the

structural compliance and failure probability respectively. Hence, the sensitivity of the constraint is crucial to the SAIP-TR. Strictly speaking, the accurate discrete variable sensitivities should be defined by the finite difference operation. However, their computational costs are usually unacceptable. In this paper, the sensitivity formulation deduced by the differential operation is adopted.

The sensitivity of the structural compliance can be derived

$$\frac{\partial C}{\partial \rho_e}=\begin{cases} -p\left(\mathbf{u}_e\right)^{\mathrm{T}}\mathbf{K}_e\mathbf{u}_e\ , \ \text{if}\ \ \rho_e=1 \\ -p\rho_{\min}^{p-1}\left(\mathbf{u}_e\right)^{\mathrm{T}}\mathbf{K}_e\mathbf{u}_e, \ \text{if}\ \ \rho_e=\rho_{\min} \end{cases} \tag{12}$$

where $\mathbf{u}_e$ is the e-th elemental displacement vector, $\mathbf{K}_e$ is the e-th elemental stiffness matrix, p = 3 is the penalization factor, and $\rho_{\min} = 10^{-3}$ is a small positive value. Here we assume that the interpolation relation between the material Young's module and the element density follows

$$E\left(\rho_e\right)=\rho_e^p E_0,\ \ \rho_e\in\{0,1\} \tag{13}$$

In the context of DPIM, the sensitivity of failure probability is

$$\begin{aligned}\frac{\partial P_f^{DPIM}}{\partial \rho_e}&=\sum_{q=1}^{N}\frac{\partial\left\{\mathcal{H}\left[-g\left(\boldsymbol{\rho},\boldsymbol{\theta}_q\right)\right]\cdot P_q\right\}}{\partial\rho_e} \\ &\approx-\sum_{q=1}^{N}\frac{1}{\sqrt{2\pi}\sigma_{\mathrm{DPIM}}}e^{-\frac{\left[g(\boldsymbol{\rho},\boldsymbol{\theta}_q)\right]^2}{2\sigma_{\mathrm{DPIM}}^2}}\frac{\partial\left[g(\boldsymbol{\rho},\boldsymbol{\theta}_q)\right]}{\partial\rho_e}P_q\end{aligned} \tag{14}$$

where the sensitivity of the performance function can be written as

$$\frac{\partial\left[g(\boldsymbol{\rho},\boldsymbol{\theta}_q)\right]}{\partial\rho_e}=-\frac{\partial\left[C(\boldsymbol{\rho},\boldsymbol{\Theta})\right]}{\partial\rho_e} \tag{15}$$

Moreover, to eliminate the checkerboard pattern and mesh-dependent phenomenon, the following linear sensitivity filter with a user-defined filter radius R is applied

$$\begin{aligned}&\frac{\overline{\partial P_f}}{\partial\rho_e}=\frac{\sum_{i=1}^{M}\omega_i\dfrac{\partial P_f^{DPIM}}{\partial\rho_e}}{\sum_{i=1}^{M}\omega_i},\ \ e=1,2,\cdots,M \\ &\omega_i=R-\mathrm{dist}(e,i),\quad \left\{i\in M\,\middle|\,\mathrm{dist}(e,i)\le R\right\}\end{aligned} \tag{16}$$

3. STRATEGY OF REDUCING COMPUTATIONAL COST

For the sake of exploring a strategy to reduce the number of representative points, we consider a cantilever beam as an example. As shown in Figure 1, two loads $\boldsymbol{F}_1$ and $\boldsymbol{F}_2$ are applied. The Poisson ratio ν = 0.3, $\bar{C}=300$, the parameters of random variables are shown in Table 1, and all variables are dimensionless. The design domain is discretized with 60×30 equal-sized Q4 elements, and 1000 representative points is selected.

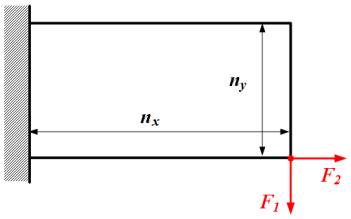

Figure 1: Design domain of the cantilever beam.

Table 1:Distributional parameters of random variables.

	Distribution	*α*	*μ*	*σ*
F_1	*Multimodal*	*(0.5,0.5)*	*(1,2)*	*(0.2,0.2)*
F_2	*Normal*	—	*1*	*0.1*
E	*Normal*	—	*1*	*0.1*

In order to find a strategy to screen the representative points that have prominent impact on the failure probability and its sensitivity, we consider the following three different designs to study the influence of different topologies on the structural compliance.

Figure 2: Three different designs for the cantilever beam.

Firstly, we rank the structural compliance corresponding to Figure 2 (a) in descending order to obtain a representative point sequence υ. Then, corresponding responses of designs in Figure 2 (b)

and Figure 2 (c) are also obtained according to sequence $\boldsymbol{\upsilon}$, and the results are shown in Figure 3.

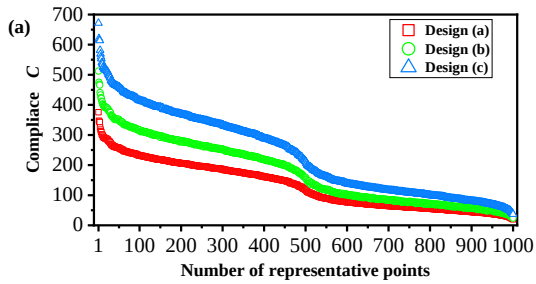

Figure 3: Structural compliance of different designs sorted by point sequence $\boldsymbol{\upsilon}$.

As can be seen from Figure 3, the compliance of design (a) presents a monotonically decreasing trend, and the compliance of other two designs show a roughly monotonically decreasing trend. Even though the compliance obtained by design (b) and design (c) are not strictly monotonically decreasing according to sequence $\boldsymbol{\upsilon}$, the overall trend is the same as design (a). Thus, the first several points in sequence $\boldsymbol{\upsilon}$ are exactly the representative points that needed to calculate the failure probability and its sensitivity. Additionally, the representative points corresponding to the worst-case under different designs are the same. The fundamental reason for the above findings is that the random variable space is invariant, and the relationship between the random load or the random Young's modulus and the compliance herein is monotonic, i.e., the greater the load, the greater the compliance, and the greater the Young's modulus, the smaller the compliance. Therefore, the representative points involved in the actual calculation can be screened out in advance and the computational cost will be reduced simultaneously.

Due to the failure probability of the structure is still zero or very small at the end of the first phase (1), the number of representative points required at this time is also very small. Therefore, at the beginning of the second phase (2), only a small number of representative points N_0 are needed to calculate the smoothing parameter σ_0 and obtain the initial sensitivity. The magnitude of N_0 is set to 100 herein. In addition, in order to support parallel computation, the following strategy in Figure 4 is proposed to adaptively update the number of representative points and calculate the smoothing parameter during the optimization.

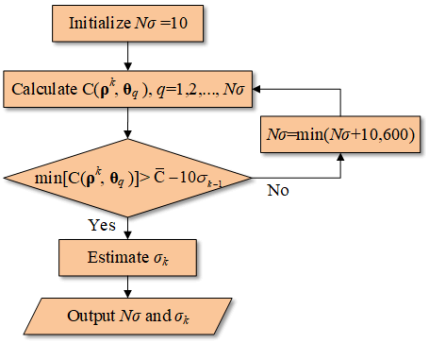

Figure 4: Flowchart of the strategy for updating the number of representative points and calculating the smoothing parameter.

4. NUMERIACAL EXAMPLES

Herein, one-half of the MBB beam, visualized in Figure 5, is considered, which is discretized into 60 × 180 equal-sized Q4 finite elements. The Poisson's ratio of the reference material v = 0.3. The distributional properties and parameters of E and F are listed in Table 2. In addition, α_r is set to be 1.25×10^{-2}, the parameter s is assigned 0.5, and the filter radius R = 2. The iterative process of topology optimization is terminated, when no further improvement of the objective function can be achieved (i.e., the mean of relative fluctuation of the objective function is less than 0.01 in 5 successive iterations) and the constraint of the failure probability is satisfied. In addition, the number of representative points N in each example is selected as 2000.

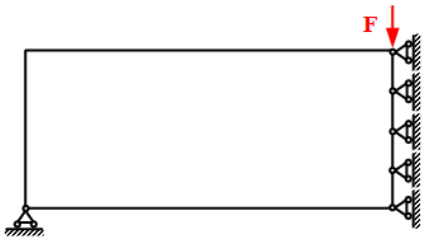

Figure 5: Design domain and boundary condition of MBB beam.

Table 2: Distributional parameters of random variables.

	Distribution	*α*	*μ*	*σ*
F (N)	*Bimodal*	*(0.5, 0.5)*	*(100, 150)*	*(10, 10)*
E (MPa)	*Normal*	—	2×10^5	2×10^4

As mentioned above, the widely adopted FORM needs to transform the random variables into standard normal variables, which causes a large error in the calculation of failure probability when the distributions of random variables are multimodal. To this end, this example firstly compares the difference between the optimized results of the proposed two-phase approach and the FORM. Herein, PMA is utilized to evaluate the failure probability. In the PMA, the mean and standard deviation of the transformed normal distribution are $\mu=\alpha_1\mu_1+\alpha_2\mu_2$=125N and $\sigma=\sqrt{\alpha_1\left(\mu_1^2+\sigma_1^2\right)+\alpha_2\left(\mu_2^2+\sigma_2^2\right)-\mu^2}$=26.93 N respectively (Hu and Du 2019). For details, the probability density function before and after transformation is shown in Figure 6. Given the threshold of failure probability and the threshold of response function as 0.01 and 4×10^{-2} J, the iteration histories of the optimization process is shown in Figure 7.

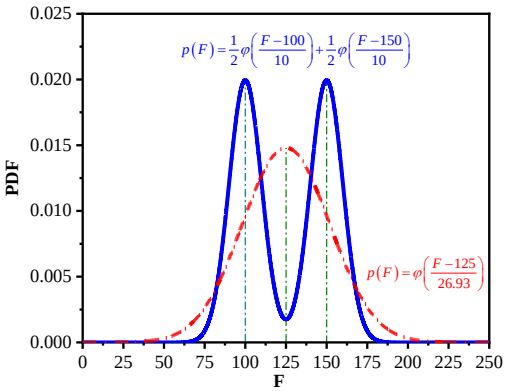

Figure 6: Probability density function curves before and after transformation.

As the iterative history shows, both methods can convergence quickly, but the optimized volume fraction is not the same. The volume fraction obtained by the PMA is larger than that acquired by the two-phase approach, and their specific volumes can be referred to Table 3. In addition, the failure probability constraint of the PMA is always satisfied, and the failure probability of the two-phase method converges to the target value gradually.

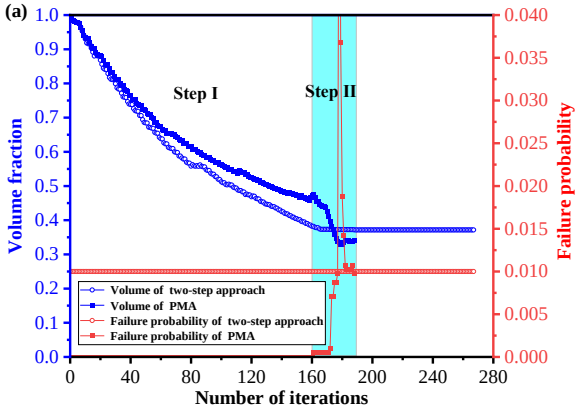

Figure 7: Iteration histories of the proposed two-phase approach and the PMA.

Table 3: Optimal results of the two-phase approach and the PMA.

Method	*Two-phase approach*	*PMA*
Volume fraction	*0.3412*	*0.3714*
P_f	*0.0097*	*0.0100*
P_f^{MCS}	*0.0094*	*0.0015*

Furthermore, the optimized results in Table 3 and Figure 8 show the topology configurations of these two methods are quite different, where more detailed features are occurred in the configuration obtained by the PMA. Moreover, compared with the verification results of MCS, the failure probability of the structure obtained by the PMA is much smaller than the target constraint value, which directly proves that it is difficult to ensure the accuracy of the results of the RBDVTO using the FORM under multimodal distributions.

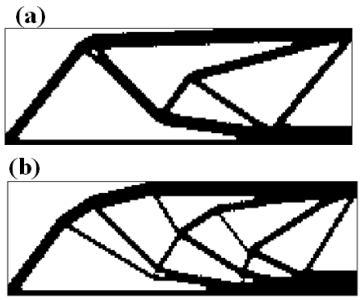

Figure 8: Topology configurations of the two-phase approach and the PMA.

In addition, this example also studies the influence of different bimodal distributions on the optimal results. Because the Gaussian mixture model is adopted to generate the multimodal distribution, different bimodal distributions can be obtained by changing the corresponding weights while the mean and standard deviation of a single Gaussian distribution are fixed. Here, three cases are discussed: (a) $\alpha_1 = 0.5$; $\alpha_2 = 0.5$, (b) $\alpha_1 = 0.4$; $\alpha_2 = 0.6$, (c) $\alpha_1 = 0.3$; $\alpha_2 = 0.7$, where α_1 and α_2 are the corresponding weights of a single Gaussian distribution respectively, and their probability density function curves are shown in the Figure 9.

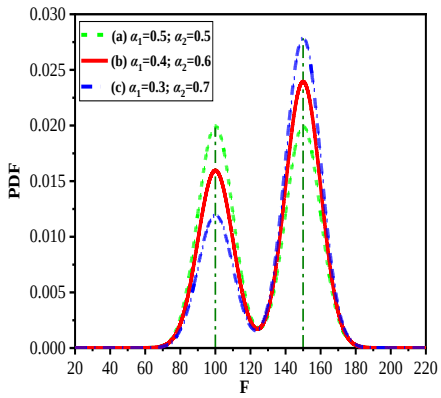

Figure 9: Probability density function curves of different weights.

According to the two-step approach, the optimized results of these three different weights are shown in Table 4 and Figure 10. These results indicate that different weights have little influence on the optimized results when the mean and standard deviation of a single Gaussian distribution are the same. Their optimized topology configurations are roughly the same, and their optimized volumes differ very little. However, the volume ratio will increase with the increment of weight α_2. This can be explained from the PDF curves in Figure 9: when the weight α_2 increases, the value at the end of the corresponding PDF curve will also augment, which means that there is a greater chance to obtain a larger load. Therefore, the optimized volume fraction will increase with the increase of the weight α_2 to ensure the safety of the structure. Moreover, all the optimized results meet the given failure probability constraints, and the accuracy of the failure probability can also be guaranteed by MCS verification.

Table 4: Optimal results of different cases

Case	*(a)*	*(b)*	*(c)*
Volume fraction	*0.3412*	*0.3413*	*0.3479*
P_f	*0.0097*	*0.0097*	*0.0092*
P_f^{MCS}	*0.0094*	*0.0094*	*0.0091*

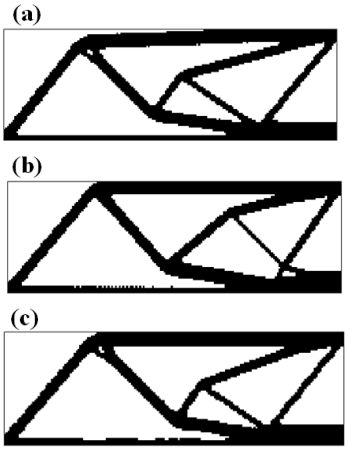

Figure 10: Topology configurations of different cases.

5. CONCLUSIONS

This paper proposes an efficient approach to reliability-based discrete variable topology optimization of continuum structures with multimodal distributions via DPIM and SAIP-TR.

In order to improve the efficiency of the optimization, a two-phase framework is

established. This framework is based on the fact that the optimized designs in the first few optimization iterations dose not fail and the finding that the compliance sorted by initial decreasing representative point sequence always maintains a roughly monotonically decreasing trend over the whole optimization process.

Numerical examples indicate that this approach can solve the RBDVTO problems efficiently and accurately. Meanwhile, due to the differences between probability density functions, the results of the RBDVTO considering unimodal and multimodal distributions are quite different, and it also confirms the necessity of the RBTO problems considering multimodal distributions. In the future, we will further extend this framework to the complex dynamic reliability-based topology optimization problems.

6. REFERENCES

Figueiredo, M. A. T., and Jain, A. K. (2002). "Unsupervised learning of finite mixture models." *IEEE Transactions on Pattern Analysis and Machine Intelligence*, 24 (3): 381–396.

Hu, Z., and Du, X.P. (2019). "Reliability methods for bimodal distribution with first-order approximation." *ASCE-ASME Journal of Risk and Uncertainty in Engineering Systems, Part B: Mechanical Engineering*, 5 (1): 1–8.

Li, L.X., Chen, G.H., Fang, M.X., and Yang, D.X. (2021). "Reliability analysis of structures with multimodal distributions based on direct probability integral method." *Reliability Engineering and System Safety*, 215 (December 2020): 107885..

Liang, Y., Sun, K., and Cheng, G.D. (2020). "Discrete variable topology optimization for compliant mechanism design via Sequential Approximate Integer Programming with Trust Region (SAIP-TR)." *Structural and Multidisciplinary Optimization*, 62 (6): 2851–2879.

Lim, H. U., and Manuel, L. (2021). "Distribution-free polynomial chaos expansion surrogate models for efficient structural reliability analysis." *Reliability Engineering and System Safety*, 205 (December 2019): 107256.

Liu, J., and Ma, Y. (2016). "A survey of manufacturing oriented topology optimization methods." *Advances in Engineering Software*, 100: 161–175.

Maute, K. (2014). "Topology optimization under uncertainty." *Topology Optimization in Structural and Continuum Mechanics*, G. I. N. Rozvany and T. Lewiński, eds., 457–471. Vienna: Springer Vienna.

Meng, X., Liu, J., Cao, L., Yu, Z., and Yang, D. (2020). "A general frame for uncertainty propagation under multimodally distributed random variables." *Computer Methods in Applied Mechanics and Engineering*, 367: 113109.

Qiu, Z.P., Huang, R., Wang, X.J., and Qi, W. (2013). "Structural reliability analysis and reliability-based design optimization: Recent advances." *Science China: Physics, Mechanics and Astronomy*, 56 (9): 1611–1618.

Valdebenito, M. A., and Schuëller, G. I. (2010). "A survey on approaches for reliability-based optimization." *Structural and Multidisciplinary Optimization*, 42 (5): 645–663.

Yan, X.Y., Liang, Y., and Cheng, G.D. (2021). "Discrete variable topology optimization for simplified convective heat transfer via sequential approximate integer programming with trust-region." *International Journal for Numerical Methods in Engineering*, 122 (20): 5844–5872.

Yao, W., Chen, X.Q., Luo, W., Van Tooren, M., and Guo, J. (2011). "Review of uncertainty-based multidisciplinary design optimization methods for aerospace vehicles." *Progress in Aerospace Sciences*, 47 (6): 450–479.

Zhang, Z., Deng, W., and Jiang, C. (2020). "Sequential approximate reliability-based design optimization for structures with multimodal random variables." *Structural and Multidisciplinary Optimization*, 62 (2): 511–528.